IAI Journals.ASM.org

Infection with *Mycobacterium avium* subsp. *paratuberculosis* Results in Rapid Interleukin-1β Release and Macrophage Transepithelial Migration

Elise A. Lamont,[a] Scott M. O'Grady,[c] William C. Davis,[d] Torsten Eckstein,[e] and Srinand Sreevatsan[a,b]

Department of Veterinary Population Medicine,[a] Department of Veterinary Biomedical Science,[b] and Department of Animal Science,[c] University of Minnesota, St. Paul, Minnesota, USA; Department of Veterinary Microbiology and Pathology, Washington State University, Pullman, Washington, USA[d]; and Department of Microbiology, Immunology and Pathology, Colorado State University, Fort Collins, Colorado, USA[e]

Pathogen processing by the intestinal epithelium involves a dynamic innate immune response initiated by pathogen-epithelial cell cross talk. Interactions between epithelium and *Mycobacterium avium* subsp. *paratuberculosis* have not been intensively studied, and it is currently unknown how the bacterium-epithelial cell cross talk contributes to the course of infection. We hypothesized that *M. avium* subsp. *paratuberculosis* harnesses host responses to recruit macrophages to the site of infection to ensure its survival and dissemination. We investigated macrophage recruitment in response to *M. avium* subsp. *paratuberculosis* using a MAC-T bovine macrophage coculture system. We show that *M. avium* subsp. *paratuberculosis* infection led to phagosome acidification within bovine epithelial (MAC-T) cells as early as 10 min, which resulted in upregulation of interleukin-1β (IL-1β) at transcript and protein levels. Within 10 min of infection, macrophages were recruited to the apical side of MAC-T cells. Inhibition of phagosome acidification or IL-1β abrogated this response, while MCP-1/CCL-2 blocking had no effect. IL-1β processing was dependent upon Ca^{2+} uptake from the extracellular medium and intracellular Ca^{2+} oscillations, as determined by EGTA and BAPTA-AM [1,2-bis(2-aminophenoxy) ethane-*N*,*N*,*N*′,*N*′-tetraacetic acid tetrakis (acetoxymethyl ester)] treatments. Thus, *M. avium* subsp. *paratuberculosis* is an opportunist that takes advantage of extracellular Ca^{2+}-dependent phagosome acidification and IL-1β processing in order to efficiently transverse the epithelium and enter its niche—the macrophage.

The intestinal epithelium is the largest surface area on humans and animals and acts as a primary barrier against pathogens (40). It is composed of a myriad of various cell types and commensal microorganisms that function together as a unique but nonseparable part of the host (22). Intestinal pathogens must overcome several mechanisms employed by the epithelium, such as mucus, secretory IgA, antimicrobial peptides, tight junctions, and the glycocalyx, to establish and promote their survival within the host (14, 15, 53). Therefore, intestinal pathogens have developed several strategies to circumvent, stun, and even manipulate the innate responses of the intestinal epithelium (4, 23, 30, 31, 39, 48).

The initial interaction between intestinal pathogens and the epithelia sets the stage for ensuing infections and may determine success, as defined by establishment, survival, and dissemination. Therefore, it is of interest to elucidate epithelium-pathogen interactions with *Mycobacterium avium* subsp. *paratuberculosis*, the causative agent of Johne's disease (JD) in ruminants (18, 51). *Mycobacterium avium* subsp. *paratuberculosis* is thought to mainly interface with macrophages despite the fact that the natural route of infection occurs via the intestinal tract (10). Like other intracellular pathogens, such as *Yersinia* spp., *Salmonella enterica* serovar Typhimurium, and *Shigella* spp., *M. avium* subsp. *paratuberculosis* infects M cells due to their lack of hydrolytic enzymes and inability to form mature phagosomes (6, 27, 28, 41, 42, 44). However, further investigations have revealed that *M. avium* subsp. *paratuberculosis* is also capable of invading enterocytes and undergoes epithelium processing and subsequent infiltration into the Peyer's patches (7, 43, 45). Studies by Patel et al. have shown that processing of *M. avium* subsp. *paratuberculosis* by bovine mammary epithelial cells (MAC-T cells) results in enhanced phagocytosis during secondary infection (34). *M. avium* subsp. *paratuberculosis* entrance into Madin-Darby bovine kidney cells (MDBK), a surrogate for intestinal epithelia, increases expression of an oxidoreductase gene (*MAP3464*) to regulate the Cdc42 pathway (2). The Cdc42 pathway is also initiated by other intracellular pathogens to form filopodia and consequent cytoskeleton rearrangement (26, 33, 58). Research utilizing the closely related bacterium *Mycobacterium avium* subsp. *avium* indicates that intestinal mycobacteria have developed several mechanisms, such as upregulation of genes related to fatty acid and membrane protein synthesis, to invade epithelium cells by a proposed regulatory role in GTP binding and modulation of bacterial cell wall structure (32). We have recently shown that *M. avium* subsp. *paratuberculosis* transcriptomes obtained from the ilea and mesenteric lymph nodes of naturally infected cattle have distinct profiles in comparison to those obtained from bovine macrophage infection (20). This dichotomy may be due to the various cell types present within the ileum and mesenteric lymph node, which further highlights the

Received 16 December 2011 **Returned for modification** 1 February 2012
Accepted 27 June 2012
Published ahead of print 9 July 2012
Editor: J. L. Flynn
Address correspondence to Srinand Sreevatsan, sreev001@umn.edu.
Supplemental material for this article may be found at http://iai.asm.org/.
Copyright © 2012, American Society for Microbiology. All Rights Reserved.
doi:10.1128/IAI.06322-11
The authors have paid a fee to allow immediate free access to this article.

importance of cell-cell cross talk during natural infection. It is likely that *M. avium* subsp. *paratuberculosis* encountered by lamina propria macrophages is significantly altered from its original state due to epithelium processing. Therefore, current research initiatives solely utilizing *M. avium* subsp. *paratuberculosis* from broth culture to infect bovine macrophages may not capture the full complexity of host-pathogen interactions and may therefore have limited utility in deciphering mycobacterial pathogenesis.

In the present study, we developed a MAC-T–bovine monocyte-derived macrophage (MDM) coculture model to investigate innate immune responses to *M. avium* subsp. *paratuberculosis* infection. We show that phagosome acidification of *M. avium* subsp. *paratuberculosis* in MAC-T cells leads to rapid processing of interleukin-1β (IL-1β). IL-1β production was determined to be critical for recruitment of MDMs to the site of *M. avium* subsp. *paratuberculosis* infection. Phagosome acidification and IL-1β transcript and protein levels were dependent upon an extracellular calcium influx. We propose that *M. avium* subsp. *paratuberculosis* takes advantage of phagosome acidification enlistment of IL-1β at the site of infection in order to efficiently transverse the epithelium and arrive at its final niche—the macrophage.

MATERIALS AND METHODS

Ethics statement. All animal work was conducted in accordance with the recommendations in the institutional guidelines and approved animal care and use committee (IACUC) protocols at the University of Minnesota (approval number 1106A01161). All other experiments were carried out in accordance with the University of Minnesota's Institutional Biosafety Committee (IBC) approved protocol number 0806H36901.

Bacterial culture. *M. avium* subsp. *paratuberculosis* strains K-10 and K-10(pWes4) expressing green fluorescent protein (GFP) were maintained in Middlebrook (MB) 7H9 medium containing 10% glycerol, 1% oleic acid-dextrose-catalase (OADC) and mycobactin J (2.0 mg/liter) (Allied Monitor, Fayette, MO) at 37°C at 120 rpm. Bacteria were subcultured at 1/10 the original culture volume once logarithmic growth was obtained (optical density at 600 nm [OD_{600}] = 1.0).

Mammalian cell culture. Monocyte-derived macrophages (MDMs) from two JD-free dairy cows (253 and 2170) were elutriated and matured as described previously (13, 19). Briefly, blood was collected from the jugular vein into a gas-sterilized vacuum container (Paragon Medical, Pierceton, IN) containing an equal volume of acid-citrate dextrose to inhibit coagulation. Blood was divided into 40-ml aliquots and centrifuged for 20 min at 2,200 rpm at room temperature. Buffy coats were collected, resuspended in 1× Dulbecco's phosphate-buffered saline (D-PBS), and layered on a 58% Percoll gradient (Sigma-Aldrich, St. Louis, MO). The monocyte layer was obtained, washed four times in 1× D-PBS, and matured in Teflon wells containing RPMI 1640 with 20% autologous serum at 37°C in a humidified chamber (5% CO_2) for 4 days. Cells were later seeded for coculture experiments. Bovine mammary epithelial cells (MAC-T) were maintained in Dulbecco's modified Eagle medium (DMEM) containing 10% fetal bovine serum (FBS) at 37°C in a humidified chamber (5% CO_2).

Conjugation of mycobacterial cell wall lipoglycans to fluorescent polystyrene beads. *M. avium* subsp. *paratuberculosis*-specific mannosylated lipoarabinomannan (ManLAM) was obtained from Eckstein (Colorado State University) (5). The following reagents were obtained through the NIH Biodefense and Emerging Infections Research Resources Repository, NIAID, NIH: *Mycobacterium tuberculosis* strain H37Rv purified lipomannan (LM) (NR-14850) and *Mycobacterium smegmatis* purified non-mannose-capped lipoarabinomannan (AraLAM) (NR-14849). Lipoglycans were purified using a previously reported method (5). Approximately 0.5 mg of ManLAM, LM, and AraLAM was separately mixed with 50 mM 2-(*N*-morpholino) ethanesulfonic acid hydrate, 4-morpholinoethanesulfonic acid (MES hydrate) buffer (pH 6.0) (Sigma-Aldrich, St. Louis, MO), and 200 μl of an aqueous suspension of fluorescein isothiocyanate (FITC)-labeled 0.1-μm carboxylate-modified microspheres (Sigma-Aldrich, St. Louis, MO) and incubated for 15 min at room temperature. Forty mg of 1-ethyl-3-(3-dimethylaminopropyl carbodiimide) (EADC) (Invitrogen, Carlsbad, CA) was added to the microsphere suspension, and the pH was adjusted to 6.5 using 0.1 N sodium hydroxide (NaOH). The reaction mixture was placed on a rocker and incubated overnight at room temperature. Lipoglycan-microsphere suspensions were quenched with 100 mM glycine, incubated for 30 min at room temperature, and washed three times using 50 mM phosphate-buffered saline (PBS) containing 0.9% sodium chloride (NaCl) at 3,000 × *g*. Lipoglycan-bound microspheres were resuspended in 5.0 ml of 50 mM PBS containing 1% BSA and 2 mM sodium azide and stored at 4°C until use in invasion assays. All microspheres were tested for successful lipoglycan binding by heating microspheres to 95°C for 10 min and subjecting the supernatants to Western blot analysis using a rabbit polyclonal antibody against whole-cell lysates of *M. avium* subsp. *paratuberculosis* (data not shown).

MAC-T–macrophage coculture and *M. avium* subsp. *paratuberculosis* invasion assay. Approximately 2.0×10^4 MAC-T cells were seeded onto the apical side of a 3.0-μm-pore-size Snapwell insert (Transwell permeable support; Corning, Lowell, MA) and incubated for 4 days in DMEM containing 10% FBS at 37°C in a humidified chamber containing 5% CO_2. Once semiconfluence was reached, the Snapwell insert was inverted and 2.0×10^4 bovine MDMs were seeded onto the new apical side. MDMs were allowed to adhere for 2 h at 37°C, and the Snapwell insert was inverted again to its original orientation, such that MAC-T cells and MDMs were located on the apical and basolateral sides of the Snapwell insert, respectively. Transwells were examined by phase-contrast microscopy to confirm macrophage adherence.

Subcultured *M. avium* subsp. *paratuberculosis* (either K-10 or GFP-expressing K-10) was grown to an OD_{600} of 0.5 (equivalent to 1.0×10^6 cells/ml) and assessed for the number of live and dead cells using a Baclight kit (Invitrogen, Carlsbad, CA) based on the manufacturer's instructions and a reported protocol (25). *M. avium* subsp. *paratuberculosis* culture was pelleted at 3,000 rpm for 10 min and washed three times in sterile PBS. The pellet was resuspended, vortexed for 5 min, and repeatedly drawn through a sterile 21-gauge needle in DMEM containing 10% FBS such that a 10:1 multiplicity of infection (MOI) was achieved. The 10:1 MOI reflected over 90% live *M. avium* subsp. *paratuberculosis* cells. Resuspended *M. avium* subsp. *paratuberculosis* was incubated for 5 min at room temperature to sediment any bacterial clumps, and the upper two-thirds of the resuspended culture was used for the invasion assay. *M. avium* subsp. *paratuberculosis* was applied to the apical chamber and allowed to infect the coculture system for 3 h at 37°C in a humidified chamber containing 5% CO_2 followed by three washings with 1× D-PBS to remove any nonadherent bacteria. The bovine MAC-T–MDMs coculture was further incubated at 37°C in a humidified chamber for 10, 30, 60, and 120 min postinfection (p.i.). The coculture was later washed using 1× D-PBS and further processed for RNA extraction, confocal imaging, or flow cytometry.

Blocking assays. The following reagents were purchased for use in blocking assays: bafilomycin A1 (Sigma-Aldrich, St. Louis, MO), bovine 9.1 IL-1β blocking antibody (provided by William C. Davis), recombinant bovine IL-1β (Thermo Scientific, Rockford, IL), human monocytic chemoattractant protein-1/CCL-2 (MCP-1) (EMD Chemicals, Gibbstown, NJ), and MCP-1/CCL-2 blocking antibody (Novus Biologicals, Littleton, CO). In order to access the role of phagosome acidification and IL-1β production, the coculture infection assay was conducted as previously stipulated with the exception of a preincubation period with either bafilomycin A1 (25 nM), 9.1 IL-1β blocking antibody (250 ng/ml or 500 ng/ml), or MCP-1/CCL-2-blocking antibody (250 ng/ml or 500 ng/ml) for 1 h at 37°C in a humidified chamber containing 5% CO_2 followed by three 1× D-PBS washes. In order to confirm MCP-1/CCL-2 blocking, a lipopolysaccharide (LPS; 1.0 μg/ml) (Sigma-Aldrich, St. Louis, MO) control was included

TABLE 1 Primers used in this study

Gene product and direction	Sequence (5′–3′)
IL–1β, F	CAATAACAAGCTGGAATTTGAGTC
IL–1β, R	TGCTTGAGAGGTGCTGATGT
MCP–1, F	CCCTCCTGTGCCTGCTACT
MCP–1, R	ATCTGGCTGAGCGAGCAC
β–actin, F	TCCTCCCTGGAGAAGAGCTA
β–actin, R	GTAGAGGTCCTTGCGGATGT

(see Fig. S1 in the supplemental material). IL-1β (200 ng/ml) was added to each coculture well in a separate bafilomycin A1 experiment to rescue MDM recruitment. MCP-1/CCL-2 (5.0 ng/ml) was added to uninfected cocultures to serve as a positive control and comparison for *M. avium* subsp. *paratuberculosis* invasion and blocking assays. All blocking assays were conducted three separate times, and the assay at each p.i. time point was performed in triplicate.

Calcium signaling assays. The following reagents were purchased for calcium signaling assays: 1,2-bis(2-aminophenoxy)ethane-*N*,*N*,*N*′,*N*′-tetraacetic acid tetrakis (acetoxymethyl ester) (BAPTA-AM) (Sigma-Aldrich, St. Louis, MO), ethyleneglycol bis (aminoethylether) tetraacetic acid (EGTA) (MP Biomedicals, Solon, OH), calcium-free DMEM (Invitrogen, Carlsbad, CA), and UTP (Sigma-Aldrich, St. Louis, MO). The MAC-T–macrophage coculture invasion assay was conducted as stated above, with the addition of either DMEM containing BAPTA-AM (25 nM) or EGTA (4 mM)-treated calcium-free DMEM alone or with UTP (25 μM) at p.i. time points. All calcium signaling assays were conducted for a total of three separate experiments using biological triplicates per p.i. time point.

RNA extraction and quantitative real-time PCR. Upon completion of p.i. time points, MAC-T cells were washed three times in 1× D-PBS, gently mixed with 1.0 ml TRIzol Reagent (Invitrogen, Carlsbad, CA), and incubated for 5 min at room temperature to ensure successful lysing. All RNA work was conducted on RNase Away (Molecular Bioproducts, San Diego, CA)-treated work surfaces. RNA was extracted per the manufacturer's instructions (Invitrogen, Carlsbad, CA) and was later treated with Turbo DNase (Ambion, Austin, TX) at 37°C for 30 min. The RNA reaction was inactivated using phenol-chloroform for 2 min at room temperature. RNA purity was assessed by measuring the 260/280 ratio obtained by NanoDrop ND-1000 (NanoDrop Products, Wilmington, DE) and the absence of amplification of the β-actin gene with direct PCR. RNA used for quantitative real-time PCR (qRT-PCR) had a minimum 260/280 ratio of 1.9. qRT-PCR of selected genes (Table 1) was conducted using a Quantifast SYBR green one-step qRT-PCR kit (Qiagen, Valencia, CA) and a Roche Light cycler 480II (Roche NimbleGen Inc., Madison, WI) with corresponding software. The following program was used: 50°C for 10 min, 95°C for 5 min, 95°C for 10 s, and 60°C for 30 s for 40 cycles. Primers were designed using Primer 3 (http://frodo.wi.mit.edu/primer3/). Fold change was calculated using the $\Delta\Delta C_T$ method and the value for the housekeeping gene, the β-actin gene, which was normalized to uninfected MAC-T cells. Products were examined on a 2% agarose gel. All samples were conducted in biological triplicates and duplicate technical replicates.

Western blot analysis. Supernatants from *M. avium* subsp. *paratuberculosis* invasion assays were collected at 10 and 30 min p.i., filtered with a 0.2-μm Millex syringe-driven filter unit (Millipore, Billerica, MA), and concentrated using a Speedvac. The following controls were included in Western blot analysis: human pro-IL-1β (Sino Biological Inc., Beijing, China), mouse IL-1β (Abcam, Cambridge, MA), and bovine IL-1β (Pierce, Rockford, IL). Twenty μl of each sample was separately combined with 5.0 μl of Laemmli buffer (Bio-Rad, Hercules, CA), denatured at 95°C, and loaded onto a Precise 4-to-20% Tris-HEPES gradient precast gel (Pierce, Rockford, IL). The gel containing processed samples was electrophoretically transferred onto a 0.2-μm-pore-size nitrocellulose membrane (Bio-Rad, Hercules, CA) for 2 h (60 V) at 4°C. The membrane was blocked overnight in 5% nonfat dried milk in 1× Tris-Tween 20 (Tris-T20; 0.1% Tween 20 [vol/vol]) buffer at 4°C. Next, the membrane was washed 5 times in 1× Tris-T20 in 5-min increments and incubated for 1 h with a 1:1,000 dilution of anti-rabbit IL-1β polyclonal antibody (Abcam, Cambridge, MA) with shaking at room temperature and further washed as previously described. The membrane was incubated with a 1:10,000 dilution of horseradish peroxidase (HRP; R&D Systems, Minneapolis, MN)-conjugated rabbit IgG (heavy plus light chain) with slight shaking at room temperature for 1 h, washed, and developed using a Western Lightning Ultra kit (PerkinElmer, Waltham, MA) per the manufacturer's instructions. The membrane was visualized using Simple_Biochemi_Acquisition from LabWorks 4.6 software (LabWorks Inc., Costa Mesa, CA).

Enzyme-linked immunosorbent assay (ELISA). Cell supernatants from both *M. avium* subsp. *paratuberculosis* invasion assays and LPS (1.0 μg/ml; control) stimulation at 10 and 30 min p.i. were analyzed for pro-IL-1β levels using a mouse IL-1β proform ELISA Ready-SET-Go! kit (Ebioscience, San Diego, CA) per the manufacturer's instructions. A standard curve was included using 2-fold dilutions of mouse pro-IL-1β. The optical density was read at 450 nm with a wavelength correction of 570 nm. All samples were loaded into triplicate wells. ELISA was repeated twice.

Dot blot analysis. Supernatants from *M. avium* subsp. *paratuberculosis* invasion and blocking assays with and without calcium were saved in 1.0-ml aliquots, filtered with 0.2-μm Millex syringe-driven filter units (Millipore, Billerica, MA), dried via Speedvac, and resuspended in 250 μl of 1× D-PBS without calcium and magnesium. One μl of each supernatant was spotted in duplicate technical replicates on a 0.45-μm-pore-size nitrocellulose membrane using the Minifold I dot blot apparatus (GE Healthcare, North America) per the manufacturer's instructions. The nitrocellulose membrane was blocked in 5% nonfat dried milk in 1× PBS-Tween 20 (PBS-T20; 0.1% T20 [vol/vol]) for 2 h at room temperature with subtle shaking, washed five times in 1× PBS-T20 at 5-min intervals, and incubated with rabbit anti-bovine IL-1β polyclonal antibody (AbD Serotec, Raleigh, NC) for 1 h at room temperature. Next, the membrane was washed as described above, incubated with goat anti-rabbit IgG-HRP (R&D systems, Minneapolis, MN), and further washed with 1× PBS-T20. The nitrocellulose membrane was developed using a Western Lightning Ultra kit (PerkinElmer, Waltham, MA) per the manufacturer's instructions and imaged under Simple_Biochemi_Acquisition from LabWorks 4.6 software (LabWorks Inc., Costa Mesa, CA). Raw density values were collected and converted to ng/ml. Concentrations were calculated based on the concentration curve for recombinant bovine IL-1β protein (Thermo Scientific, Rockford, IL).

Lactate dehydrogenase cytotoxicity assay. A lactate dehydrogenase (LDH) cytotoxicity assay was performed on MAC-T cells infected with *M. avium* subsp. *paratuberculosis* as stipulated by the manufacturer (Clontech, Mountain View, CA). Briefly, 100 μl containing 4.0×10^5 MAC-T cells/ml in DMEM with 1% BSA was seeded into an optically clear 96-well microtiter plate and allowed to adhere overnight at 37°C in a humidified chamber containing 5% CO_2. Medium was removed, and all cells were washed three times with 1× D-PBS to remove spontaneously released LDH. *M. avium* subsp. *paratuberculosis* invasion of MAC-T cells was performed as described above with the exception of 1% BSA in placement of 10% FBS. The following controls were included: background (medium alone), low LDH release (uninfected cells in medium; spontaneous release of LDH), high LDH release (2% Triton X-100), *M. avium* subsp. *paratuberculosis* alone, and LPS (1.0 μg/ml). Optical density was recorded at 490 nm with an applied correction at 600 nm. Optical density readings were converted to LDH microunits based on a generated standard curve. Assays at all time points were conducted in triplicate. The LDH assay was repeated a total of three times.

Cell staining and confocal microscopy. All cells were allowed to adhere to glass coverslips (no. 1.5 thickness) in 24 well plates. Phagosome acidification staining was based in part on a previously reported protocol (25). Upon the final 30 min after infection of MAC-T cells, 25 nM Lyso-

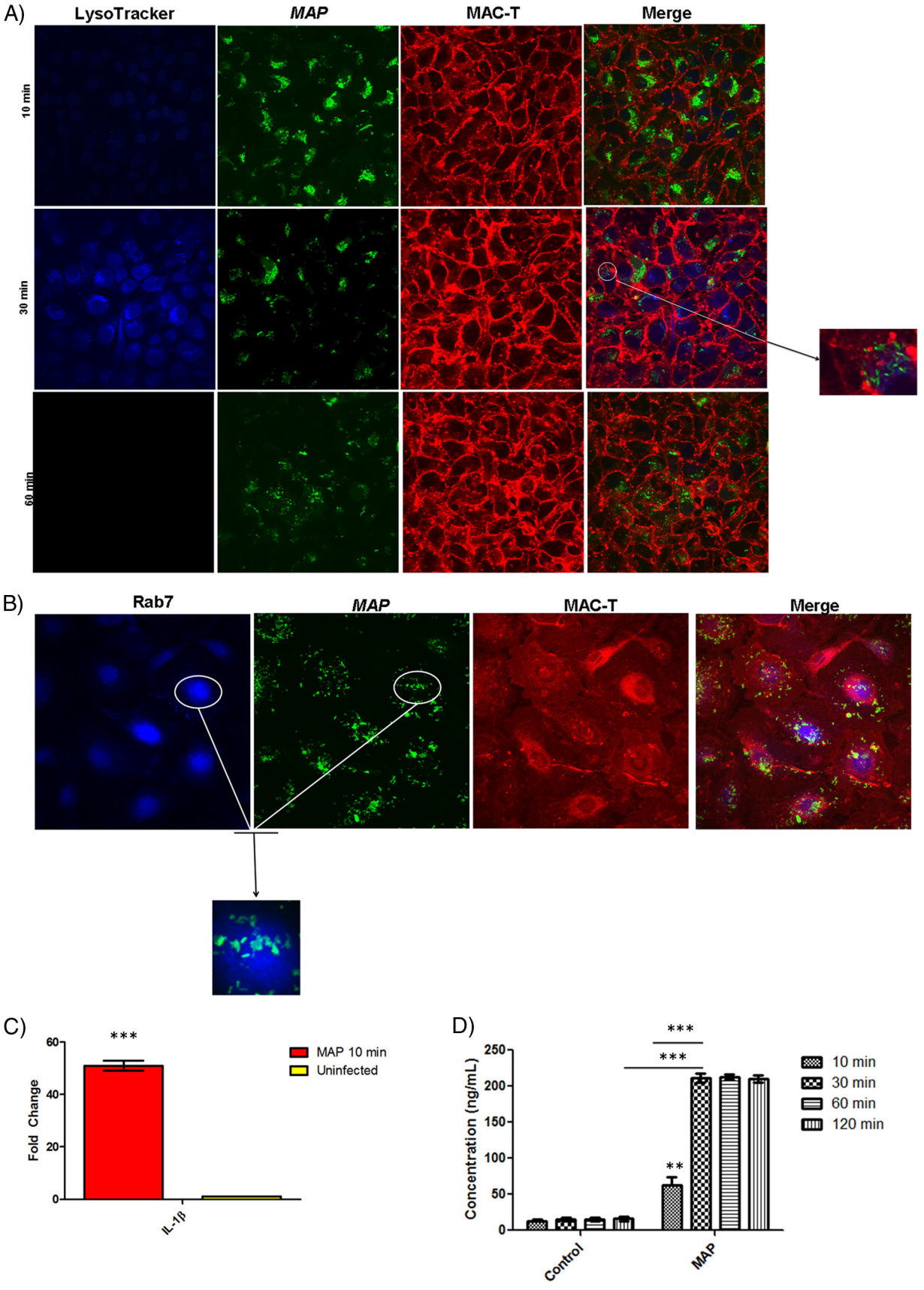
A)
LysoTracker
MAP
MAC-T
Merge
10 min
30 min
60 min
B)
Rab7
MAP
MAC-T
Merge
C)
***
MAP 10 min
Uninfected
Fold Change
60
40
20
0
IL-1β
D)
***
***
**
Concentration (ng/mL)
250
200
150
100
50
0
10 min
30 min
60 min
120 min
Control
MAP

Tracker blue (Invitrogen, Carlsbad, CA) was added to culture medium and incubated at 37°C in a humidified chamber with 5% CO_2. After the designated p.i. time point was completed, culture medium was decanted and cells were washed three times in 1× D-PBS. MAC-T cells were stained in prewarmed (37°C) Deep Red CellMask plasma membrane stain (2.5 μg/ml) (Invitrogen, Carlsbad, CA) for 5 min and washed three times in 1× D-PBS. Coverslips were removed, and cells were immediately fixed in absolute methanol for 5 min at −20°C followed by two washes with ice-cold 1× D-PBS. In a separate experiment examining Rab7 expression, MAC-T cells were fixed in 2% paraformaldehyde at 37°C for 5 min, rinsed in PBS containing 0.01% bovine serum albumin (BSA), permeabilized in ice cold methanol at −20°C for 5 min, and blocked with PBS containing 1% BSA for 1 h at room temperature. MAC-T cells were further incubated with 1:500 anti-mouse Rab7 monoclonal antibody (Abcam, Cambridge, MA) for 1 h at 37°C in a humidified chamber containing 5% CO_2, rinsed three times in PBS, and stained with 1:1,000 Alexa Fluor 405 goat anti-mouse IgG (Invitrogen, Carlsbad, CA) for 1 h at room temperature in the dark. Coverslips were mounted on glass slides using Prolong gold reagent (Invitrogen, Carlsbad, CA) and sealed with nail polish. All slides were stored at 4°C until confocal imaging.

Coculture Transwells were preprocessed by a method similar to the Rab7 staining in MAC-T cells. Transwells were incubated with a 1:500 dilution of rabbit anti-bovine CD11b (Abcam, Cambridge, MA) and mouse anti-bovine cytokeratin (Abcam, Cambridge, MA) for 2 h at 37°C in a humidified chamber (5% CO_2). Subsequently, cells were washed three times with 1× D-PBS, incubated with 1:1,000 dilutions of Alexa Fluor 405 goat anti-mouse IgG and Alexa Fluor 680 donkey anti-rabbit IgG (Invitrogen, Carlsbad, CA) for 1 h at room temperature in the dark, and rinsed three times in 1× D-PBS. Transwells were removed by scoring the support circumference with an 18.5-gauge needle, mounted on glass coverslips, and stored as described above.

The supernatant from the apical chamber was saved and transferred to 24-well plates containing glass coverslips in order to recover any recruited macrophages. Macrophages were incubated in RPMI 1640 containing amikacin (200 μg/ml) (Sigma-Aldrich, St. Louis, MO) for 2 h at 37°C in a humidified chamber (5% CO_2) to remove extracellular bacteria and subsequently stained and fixed using the CellMask protocol described above.

All slides were imaged using the Olympus Fluoview 1000 upright confocal microscope (Olympus, South-end-on-sea, Essex, United Kingdom). The following lasers were used to visualize cells: Alexa Fluor 405, FITC, Cy5, and/or DAPI (4′,6-diamidino-2-phenylindole). A Z series for each slide was collected in 1.0-μm steps and stacked to render a complete image. Three fields per slide were visualized.

Fluorescence-activated cell sorting analysis. Upon completion of p.i. time points from *M. avium* subsp. *paratuberculosis* invasion assays, supernatants were collected from the apical chamber, centrifuged at 1,200 rpm, and washed three times using sterile PBS. The pelleted cells were resuspended in 500 μl of PBS, blocked using 1× PBS containing 1% BSA for 1 h on ice, and immediately washed three times with PBS. Cells were incubated separately with 1:500 dilutions of phycoerythrin (PE)-conjugated anti-human CD14 (R&D Systems, Minneapolis, MN) and anti-bovine CD11b-FITC (Raybiotech Inc., Norcross, GA) primary antibodies or appropriate isotype controls (R&D Systems, Minneapolis, MN) for 1 h on ice and washed three times with PBS between stainings. Flow-cytometric analysis was conducted using a FACSCanto equipped with FACSDiva software (BD Biosciences, San Jose, CA). Bovine MDMs were defined as $CD11b^{hi}$ ($FITC^{hi}$) and $CD14^{hi}$ (PE^{hi}). Cell population was recorded at 10,000 events. Experiments were conducted three times using triplicate biological samples (per p.i. time point).

Graphs and statistical analyses. Percent colocalization of LysoTracker staining and FITC was examined and calculated based on 20 randomly selected fields using the overlapping coefficient in Fluoview 1000 software (Olympus, South-end-on-sea, Essex, United Kingdom). All graphs were generated using GraphPad Prism software (GraphPad Software, La Jolla, CA). Means and standard errors of the means (SEM) were calculated. qRT-PCR and dot blot results were analyzed using a two-way analysis of variance (ANOVA) with Bonferroni correction. *P* values of less than 0.01 were considered statistically significant.

RESULTS

***M. avium* subsp. *paratuberculosis* phagosome acidification leads to interleukin-1β secretion at the epithelial interface not due to cell death.** In order to assess the innate response induced by epithelium-*M. avium* subsp. *paratuberculosis* interaction, we infected MAC-T cells with a GFP-expressing strain of *M. avium* subsp. *paratuberculosis* K-10 and imaged the cells using confocal microscopy. *M. avium* subsp. *paratuberculosis* K-10 infection resulted in early phagosome acidification within 10 min p.i. and reached peak LysoTracker fluorescence intensity by 30 min (Fig. 1A). This is in stark contrast to ManLAM, a mycobacterial cell wall lipoglycan responsible for phagosome maturation arrest, which did not display LysoTracker staining throughout the infection (see Fig. S2 in the supplemental material) (9). Phagosome acidification was sustained in AraLAM-, LM-, and carboxylate-modified microsphere controls, while *M. avium* subsp. *paratuberculosis*-guided phagosome acidification dissipated by 1 h p.i. (see Fig. S2A and B). Phagosome acidification was validated by staining for the late endosomal marker Rab7 during the infection process (Fig. 1B). This observation is surprising, as pathogenic mycobacteria have developed several strategies to shut off the acidification process (9, 21, 47, 54, 55, 56). It is important to note that these previous studies were conducted with macrophages; therefore, a different cell type, like the epithelium, may function differently in response to mycobacteria. We found that IL-1β transcription in MAC-T cells showed a 50-fold upregulation compared to uninfected controls by 10 min p.i., which corresponded to *M. avium* subsp. *paratuberculosis*-induced phagosome acidification (Fig. 1C). IL-1β transcript levels were validated for activation by Western blot analysis and the absence of pro-IL-1β (see Fig. S3). IL-1β protein concentration was also determined via immunoblotting. MAC-T cells show maximum IL-1β production (~200 ng/ml) by 30 min p.i. that also coincides with peak LysoTracker intensity (Fig. 1D). Although IL-1β has been reported to be an integral component for host defense, it may also serve as a chemoattractant for macrophages and has previously been identified to be an integral cytokine in granuloma formation during mycobacteriosis (29, 35, 57). Therefore, *M. avium* subsp. *paratuberculosis* may take advantage of the epithelium IL-1β response to

FIG 1 *M. avium* subsp. *paratuberculosis* (MAP) induces phagosome acidification and IL-1β processing at the epithelium interface. (A) Confocal microscopy of phagosome acidification in MAC-T cells. MAC-T cells were assessed for phagosome acidification at 10, 30, and 60 min after infection with *M. avium* subsp. *paratuberculosis* using LysoTracker blue. Approximately 60% of MAC-T cells contained *M. avium* subsp. *paratuberculosis*. *M. avium* subsp. *paratuberculosis* induced phagosome acidification at 10 and 30 min postinfection but ceased at 60 min postinfection. (B) Rab7 stain of MAC-T cells infected with *M. avium* subsp. *paratuberculosis* 30 min postinfection. LysoTracker staining was validated with indirect staining for the late endosomal marker Rab7. Infected MAC-T cells were positive for Rab7. (C) qRT-PCR of uninfected and infected MAC-T cells at 10 min postinfection. In stark contrast to uninfected cells, *M. avium* subsp. *paratuberculosis*-infected MAC-T cells showed a 50-fold upregulation of IL-1β. (D) IL-1β protein levels in uninfected and infected MAC-T cells. Infected MAC-T cells reached peak IL-1β expression at 30 min postinfection. **, $P < 0.01$; ***, $P < 0.001$.

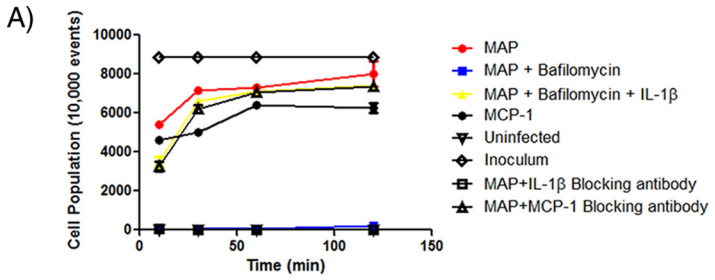
A)
Cell Population (10,000 events)
10000
8000
6000
4000
2000
0
0
50
100
150
Time (min)
MAP
MAP + Bafilomycin
MAP + Bafilomycin + IL-1β
MCP-1
Uninfected
Inoculum
MAP+IL-1β Blocking antibody
MAP+MCP-1 Blocking antibody

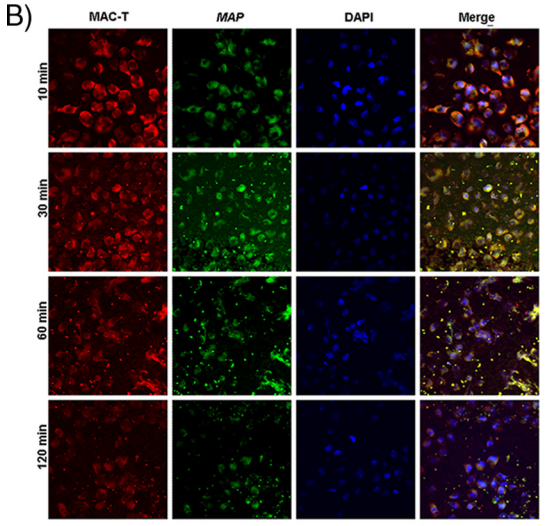
B)
MAC-T
MAP
DAPI
Merge
10 min
30 min
60 min
120 min

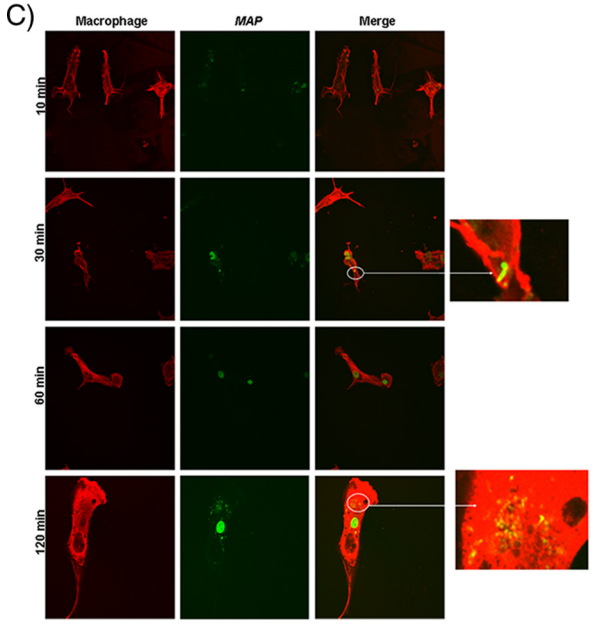
C)
Macrophage
MAP
Merge
10 min
30 min
60 min
120 min

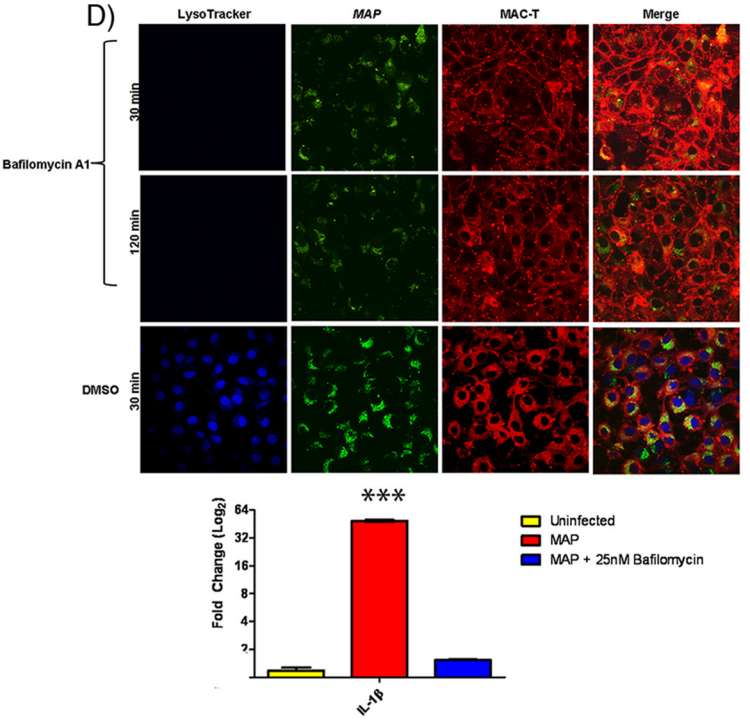
D)
LysoTracker
MAP
MAC-T
Merge
Bafilomycin A1
30 min
120 min
DMSO
30 min
***
Fold Change (Log2)
64
32
16
8
4
2
IL-1β
Uninfected
MAP
MAP + 25nM Bafilomycin

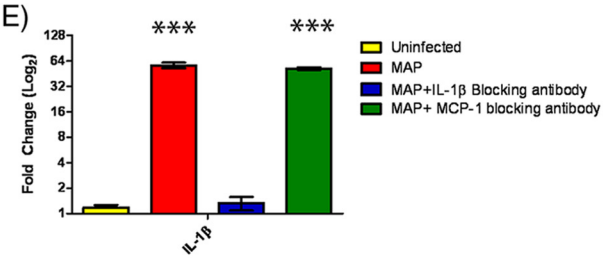
E)
***
***
Fold Change (Log2)
128
64
32
16
8
4
2
1
IL-1β
Uninfected
MAP
MAP+IL-1β Blocking antibody
MAP+ MCP-1 blocking antibody

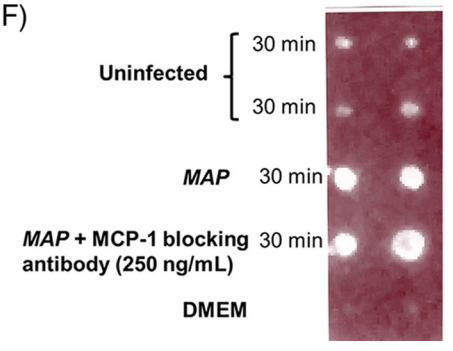
F)
Uninfected
30 min
30 min
MAP
30 min
MAP + MCP-1 blocking antibody (250 ng/mL)
30 min
DMEM

recruit macrophages to the site of infection to ensure its survival and dissemination.

Phagosome acidification and IL-1β production are necessary for macrophage transepithelial migration and *M. avium* subsp. *paratuberculosis* escape from the epithelium. We next investigated macrophage recruitment during *M. avium* subsp. *paratuberculosis* infection in a MAC-T–bovine MDM coculture system. MAC-T cells and MDMs adhered to the apical and basolateral sides of Transwells, respectively. If MDM recruitment to the site of infection was induced by *M. avium* subsp. *paratuberculosis*, MDMs should permeate the Transwell pores and reside within the apical chamber of the coculture system (Fig. 2). MDM recruitment was assessed by flow cytometry of apical-chamber supernatants. *M. avium* subsp. *paratuberculosis* infection in MAC-T cells led to recruitment of MDMs (5,000 cells/10,000 recorded events) into the apical chamber within 10 min (Fig. 2A, B, And C). The entire MDM cell population permeated into the apical chamber by 120 min and was comparable to extravasation in the MCP-1 control treatment (Fig. 2A). Confocal microscopy confirmed *M. avium* subsp. *paratuberculosis* escape from MAC-T cells and phagocytosis into MDMs during the migration process (Fig. 2B and C). Next, we sought to determine the role of phagosome acidification in the *M. avium* subsp. *paratuberculosis* promoted macrophage transepithelial migration. We pretreated MAC-T cells prior to *M. avium* subsp. *paratuberculosis* infection with bafilomycin A1, an established inhibitor of vacuolar ATPases, to block the acidification process (Fig. 2D). Bafilomycin A1 treatment resulted in a complete abrogation of MDM recruitment (Fig. 2A). Furthermore, bafilomycin A1 treatment prevented the production of IL-1β and was comparable to transcript levels in uninfected MAC-T cells (Fig. 2D). Since the production of IL-1β may be critical to macrophage transepithelial migration, we supplemented the bafilomycin A1 treatment with the exact concentration of IL-1β secreted during normal infection. Addition of IL-1β restored MDM migration to the apical chamber in cell numbers comparable to those seen with *M. avium* subsp. *paratuberculosis* infection alone (Fig. 2A). Furthermore, inhibition of IL-1β by a blocking antibody abrogated macrophage recruitment (Fig. 2A and E). Despite the apparent macrophage recruitment reliance on IL-1β, an alternative may be that another chemoattractant induced IL-1β production and is actually responsible for transepithelial migration. For example, Gavrilin et al. have shown that MCP-1 upregulates IL-1β expression in monocytes (17). Therefore, we included an MCP-1-blocking antibody pretreatment to *M. avium* subsp. *paratuberculosis* infection in the coculture system. MCP-1 did not affect macrophage recruitment or IL-1β transcript and protein levels (Fig. 2A, E, And F). Although the above data implicated IL-1β recruitment of macrophages, they did not rule out the possibility that this was a direct effect. In other words, the potential remained that IL-1β was a result of *M. avium* subsp. *paratuberculosis*-induced cytotoxicity, which may have led to the destruction of the MAC-T monolayer integrity and removed a barrier for the macrophages to cross. In order to determine the potential for cell death caused by *M. avium* subsp. *paratuberculosis* infection, we analyzed cell culture supernatants 10 and 30 min p.i. In contrast to the results obtained with treatment with 2% Triton X-100, lactate dehydrogenase (LDH) release in *M. avium* subsp. *paratuberculosis*-infected cells was not elevated compared to the uninfected control (see Fig. S4B in the supplemental material). LDH data determined that IL-1β presence in cell culture supernatants was not a result of cell content release due to necrosis but is indicative of secretion from viable MAC-T cells. Taken together, these data indicate that phagosome acidification promotes IL-1β expression, which is the critical component leading to macrophage transepithelial migration.

Phagosome acidification and IL-1β expression are dependent upon an extracellular calcium flux. Phagosome maturation into the lysosome requires calcium oscillations; therefore, we asked whether this flux originated from the extracellular milieu or intracellular stores. It is also important to note that transepithelial migration is also dependent upon calcium signaling (11). We treated MAC-T cells with BAPTA-AM, a chelator of calcium from intracellular and extracellular sources, during *M. avium* subsp. *paratuberculosis* infection. BAPTA-AM treatment abolished both phagosome acidification and upregulation of IL-1β (Fig. 3A and B). Removal of calcium from the extracellular environment using EGTA-treated calcium-free medium also blocked phagosome acidification and IL-1β expression (Fig. 3B, C, And D). Furthermore, UTP supplementation restored phagosome acidification in the calcium-free EGTA medium treatment, which indicates that intracellular stores were still functional (Fig. 3E). Thus, *M. avium* subsp. *paratuberculosis* preferentially utilizes an extracellular calcium flux in order to complete phagosome acidification and IL-1β production.

DISCUSSION

The intestinal epithelium serves as a gatekeeper that allows for nutrient absorption and luminal sampling but blocks microbial (both commensal and pathogen) passage (40). Therefore, intracellular pathogens that target host cells within the gastrointestinal tract, particularly those cells that reside within the lamina propria, have developed exquisite and complex mechanisms to overcome this barrier (32, 48). The defining features of *M. avium* subsp. *paratuberculosis* infection in ruminants are lesions and noncaseating granulomas present in the intestinal wall; however, there remains a paucity of studies investigating how *M. avium* subsp.

FIG 2 *M. avium* subsp. *paratuberculosis* (MAP) enlistment of IL-1β-recruited macrophages to the initial site of infection. (A) FACS analysis of macrophage recruitment in response to *M. avium* subsp. *paratuberculosis* infection in the epithelium-bovine macrophage coculture system. *M. avium* subsp. *paratuberculosis* infection readily recruits macrophages to the apical chamber. Macrophage recruitment was abolished when phagosome acidification was blocked with bafilomycin A1 or IL-1β expression was prevented. Recruitment was rescued in bafilomycin A1 treatment with the addition of recombinant IL-1β protein. MCP-1 blocking did not impact macrophage recruitment. (B and C) Confocal microscopy of a coculture infection with *M. avium* subsp. *paratuberculosis*. (B) Macrophages are readily recruited to the apical chamber, as the Transwell contained only MAC-T cells. (C) Macrophages were found only in the apical chamber. Recruited macrophages contained *M. avium* subsp. *paratuberculosis*. (D) Bafilomycin A1 treatment abrogated phagosome acidification and IL-1β transcription (qRT-PCR). Confocal microscopy of bafilomycin A1 treated cells and vehicle control (DMSO) (top). Bafilomycin A1 treatment blocked IL-1β transcription, and results are indistinguishable from those of uninfected controls (bottom). (E) qRT-PCR of infected MAC-T cells treated with IL-1β blocking antibody or MCP-1 blocking antibody. MCP-1 blocking does not impact IL-1β expression. (F) IL-1β dot blot. Cell supernatants were collected during *M. avium* subsp. *paratuberculosis* infection of MAC-T cells. The addition of the MCP-1 blocking antibody did not influence IL-1β protein levels. ***, $P < 0.001$.

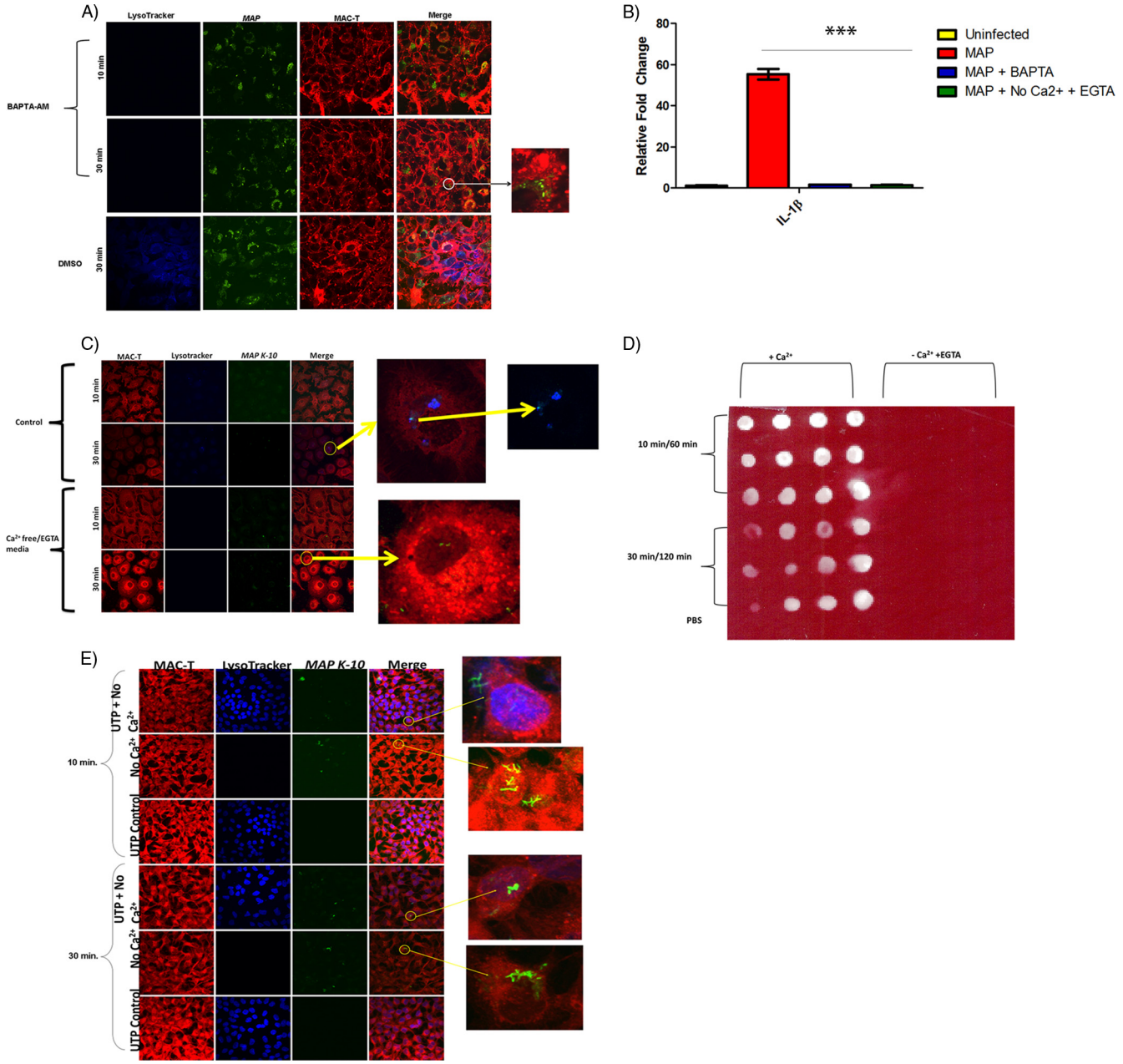

FIG 3 *M. avium* subsp. *paratuberculosis*-induced phagosome acidification and IL-1β processing is dependent upon an extracellular calcium flux. (A) Confocal microscopy of BAPTA-AM-treated MAC-T cells during *M. avium* subsp. *paratuberculosis* infection. BAPTA-AM abolished LysoTracker staining. (B) qRT-PCR of infected MAC-T cells treated with BAPTA-AM and calcium-free EGTA medium. BAPTA-AM and calcium-free medium prevented IL-1β transcription. (C) Confocal microscopy of infected MAC-T cells treated with calcium-free EGTA medium 10 and 30 min postinfection. Calcium-free EGTA medium abrogated LysoTracker staining. (D) IL-1β dot blot of infected MAC-T cells treated with calcium-free EGTA medium. The addition of calcium-free EGTA medium prevented IL-1β expression at all postinfection time points. (E) Confocal microscopy of combined UTP and calcium-free treatment in infected MAC-T cells 10 min and 30 min p.i. The addition of UTP to calcium-free treatment restored phagosome acidification. Therefore, intracellular calcium stores remained functional. ***, $P < 0.001$.

paratuberculosis interacts with the epithelium. Given that the intestinal epithelium is the first host tissue that *M. avium* subsp. *paratuberculosis* comes into contact with, it is likely that the intestinal epithelium might play an important role in facilitating infection (10, 18). For example, in a 1996 study, Alzuherri et al. reported monocyte/macrophage infiltration into the intestinal mucosa of *M. avium* subsp. *paratuberculosis*-infected Scottish Blackface ewes as well as elevated levels of IL-1β (3). To our knowledge, this is the first study to elucidate the mechanism behind Alzuherri and colleagues' observations utilizing a novel MAC-T–bovine macrophage coculture system during *M. avium* subsp. *paratuberculosis* infection. This is also the first report to define *M. avium* subsp. *paratuberculosis*-directed macrophage recruitment to the infection site due to phagosome acidification and

IL-1β production. The MAC-T–bovine macrophage coculture system not only takes advantage of epithelium processing of *M. avium* subsp. *paratuberculosis* but also takes into account the nuances of cell-to-cell cross talk that takes place during infection. This novel mechanism of host establishment may also explain transepithelial migration observed in other phagosomal bacteria, such as *Brucella* spp. For instance, Ackermann et al. noted transepithelial migration of *Brucella abortus* into neutrophils and macrophages in a calf ligated ileal loop model (1). This dynamic process at the epithelium interface may ultimately determine pathogen success.

Although epithelium-*M. avium* subsp. *paratuberculosis* interactions may seem a bedlam of host and pathogen signals, the results of the present study suggest that these signals are orchestrated and synchronized in a manner that promotes pathogen establishment and survival. Previous studies have shown that *M. avium* subsp. *paratuberculosis* exposure to a hyperosmolar environment, like that found within epithelial cells, enhances phagocytosis during secondary infection (34). Furthermore, *M. avium* subsp. *paratuberculosis* entrance into the epithelium mirrors that of other intestinal pathogens in that there appears to be an upregulation of pathways involved in cytoskeleton rearrangement (2). The closely related pathogen *Mycobacterium avium* subsp. *avium* has been reported to upregulate a number of genes related to fatty acid and membrane protein synthesis in HEp-2 cells (32). Therefore, it is likely that *M. avium* subsp *paratuberculosis* has developed certain signaling mechanisms to survive within the intestinal epithelium. We show that infection with *M. avium* subsp. *paratuberculosis* in MAC-T cells leads to phagosome acidification and rapid IL-1β expression from viable cells. Phagosome acidification may seem to be a contradiction to *M. avium* subsp. *paratuberculosis*' major goal of survival, as it is well documented that pathogenic mycobacteria employ numerous mechanisms to inhibit the acidification process (37, 50, 52, 56). However, a recent report by Koo et al. suggests that phagosome acidification may actually serve as an effective survival and dissemination strategy (24). Koo et al. have shown that phagosome acidification aids in IL-1β processing during lysosomal disruption (24). Furthermore, IL-1β may serve as a chemoattractant for macrophages and is also reported to be a necessary cytokine in granuloma formation and maintenance (29, 35, 36, 57). We propose that the intestinal epithelium represents a transition cell for *M. avium* subsp. *paratuberculosis* based on data indicating that *M. avium* subsp. *paratuberculosis* replicates inefficiently within this tissue (7, 34). *M. avium* subsp. *paratuberculosis* temporarily resides within the epithelium while macrophage recruitment is elicited by phagosome acidification and IL-1β expression and release by the epithelium. Once macrophages arrive at the site of infection, *M. avium* subsp. *paratuberculosis* enters the cells and begins proliferation and dissemination to other locations within the host. We show that *M. avium* subsp. *paratuberculosis* infection causes MDM recruitment to the primary site of infection (MAC-T cells) in a coculture system. Macrophage transepithelial migration requires phagosome acidification and IL-1β expression, and these two events are not mutually exclusive. IL-1β is the true chemoattractant agent responsible for this mechanism, since blocking of a previously reported linked chemoattractant, MCP-1/CCL-2, failed to abrogate macrophage recruitment and IL-1β processing.

Transepithelial migration may also be an important survival and establishment strategy in other pathogenic mycobacteria. Bermudez et al. developed a two-layer Transwell system containing A549 alveolar epithelial cells and endothelial cells to investigate monocyte translocation during infection with *M. tuberculosis* H37Rv, *M. avium* 101, and *Mycobacterium bovis* BCG strain Pasteur (8, 34). Passage through alveolar epithelial cells increased *M. tuberculosis* translocation across the bilayer compared to direct endothelial infection, which indicates that exposure to alveolar epithelial cells allowed the emergence of an *M. tuberculosis* invasive phenotype (8). Mycobacterial invasion in alveolar epithelial cells also enhanced monocyte migration across the bilayer (8). One briefly mentioned observation was the decrease in transmembrane resistance (TER), which may have influenced monolayer integrity. Interestingly, reduction in the TER has been observed in intestinal epithelium cells infected with *Salmonella enterica* serovar Typhimurium and *Shigella flexneri* (23, 39). The diminished TER is a result of dephosphorylated occludin and degradation of zona occludens 1, which promoted the migration of neutrophils to the apical side of the epithelium. It is possible that the TER reduction observed by Bermudez et al. may be due to a similar mechanism of tight junction protein degradation. One limitation of our study is that MAC-T cells form low resistance or diffuse tight junctions. These tight junctions presumably offered less of an impediment for macrophages to transverse the monolayer into apical chamber. Ongoing studies in our laboratory are using a bovine intestinal epithelial (BIE) cell line, which forms higher-resistance junctions, to determine if the reduction in TER noted by Bermudez et al. also occurs with *M. avium* subsp. *paratuberculosis* infection (8).

Phagosome acidification and IL-1β expression were found to be dependent on an extracellular calcium influx. Calcium plays a dual role as it aids in phagolysosome fusion and is necessary for the development of pro-IL-1β into its mature form (16, 38). Additionally, calcium fluxes are necessary for leukocyte and macrophage transepithelial migration (11, 12). The epithelium responds to *M. avium* subsp. *paratuberculosis* infection by preferentially inducing a calcium influx from the extracellular medium. Targeting of the transport mechanism responsible for calcium influx by an appropriate blocker may provide a novel prophylactic for Johne's disease. It is likely that functional disruption of this transport pathway will prevent IL-1β expression by the host during *M. avium* subsp. *paratuberculosis* infection and consequently macrophage recruitment to the epithelium. For example, P2X receptors have been linked to calcium influx from the extracellular milieu and are currently under consideration as potential therapeutic targets for inflammation-based neurodegenerative disorders (46, 49). Also, the connection between extracellular calcium, phagosome maturation, IL-1β, and macrophage recruitment may be exploited in *M. avium* subsp. *paratuberculosis* vaccine candidate screening. Attenuation may be detected and candidates worthy of future experimentation identified by the abrogation of calcium influx and phagosome acidification at the epithelium interface. More importantly, our MAC-T–MDM coculture model provides a useful system to investigate *M. avium* subsp. *paratuberculosis* vaccine candidates.

In conclusion, we demonstrate that *M. avium* subsp. *paratuberculosis* infection promotes a cooperative self-destruction state in the host epithelium, which entails maturation of the phagosome and IL-1β production that is dependent upon extracellular

calcium. IL-1β in turn is available to act as a chemoattractant for macrophages, which supply an escape route for *M. avium* subsp. *paratuberculosis*. Although these results were identified in an *in vitro* system, they may also be applied to natural infection. Ongoing studies in our laboratory seek to define which *M. avium* subsp. *paratuberculosis* effector molecules may play a role in phagosome acidification and escape from the epithelium. Thus, IL-1β, which is most widely known as a critical cytokine for control of pathogenic mycobacteria, may paradoxically promote pathogen establishment and dissemination within the host.

ACKNOWLEDGMENTS

We thank Raul G. Barletta (University of Nebraska-Lincoln) and Luiz E. Bermudez (Oregon State University) for their generous gifts of GFP-expressing *M. avium* subsp. *paratuberculosis* strain K-10 and MAC-T cells, respectively. We thank John P. Bannantine (U.S. Department of Agriculture) for providing the rabbit polyclonal antibody against *M. avium* subsp. *paratuberculosis*. We acknowledge the help of the University of Minnesota's bovine blood collection service.

This study was supported by USDA-CRIS (MIN-62-027), USDA-CSREES NRI (2005-35204-16106), and University of Minnesota College of Veterinary Medicine Agriculture Research Station (1802-11646-AES0062027) grants awarded to S.S.

REFERENCES

1. **Ackermann MR, Cheville NF, Deyoe BL.** 1988. Bovine ileal dome lymphoepithelial cells: endocytosis and transport of Brucella abortus strain 19. Veterinary Pathol. **25**:28–35.
2. **Alonso-Hearn M, Patel D, Danelishvili L, Meunier-Goddik L, Bermudez LE.** 2008. The Mycobacterium avium subsp. paratuberculosis MAP3464 gene encodes an oxidoreductase involved in invasion of bovine epithelial cells through the activation of host cell Cdc42. Infect. Immun. **76**:170–178.
3. **Alzuherri HM, Woodall CJ, Clarke CJ.** 1996. Increased intestinal TNF-alpha, IL-1 beta and IL-6 expression in ovine paratuberculosis. Vet. Immunol. Immunopathol. **49**:331–345.
4. **Ashida H, et al.** 2010. Shigella deploy multiple countermeasures against host innate immune responses. Curr. Opin. Microbiol.
5. **Basler T, et al.** 2010. TNF- expression in RAW264.7 macrophages infected with pathogenic mycobacteria: evidence for an involvement of lipomannan. J. Leukocyte Biol. **87**:173.
6. **Baumler AJ, Tsolis RM, Valentine PJ, Ficht TA, Heffron F.** 1997. Synergistic effect of mutations in invA and lpfC on the ability of Salmonella typhimurium to cause murine typhoid. Infect. Immun. **65**:2254–2259.
7. **Bermudez LE, Petrofsky M, Sommer S, Barletta RG.** 2010. Peyer's patch-deficient mice demonstrate that Mycobacterium avium subsp. paratuberculosis translocates across the mucosal barrier via both M cells and enterocytes but has inefficient dissemination. Infect. Immun. **78**:3570–3577.
8. **Bermudez LE, Sangari FJ, Kolonoski P, Petrofsky M, Goodman J.** 2002. The efficiency of the translocation of Mycobacterium tuberculosis across a bilayer of epithelial and endothelial cells as a model of the alveolar wall is a consequence of transport within mononuclear phagocytes and invasion of alveolar epithelial cells. Infect. Immun. **70**:140–146.
9. **Briken V, Porcelli SA, Besra GS, Kremer L.** 2004. Mycobacterial lipoarabinomannan and related lipoglycans: from biogenesis to modulation of the immune response. Mol. Microbiol. **53**:391–403.
10. **Chacon O, Bermudez LE, Barletta RG.** 2004. Johne's disease, inflammatory bowel disease, and Mycobacterium paratuberculosis. Annu. Rev. Microbiol. **58**:329–363.
11. **Chun J, Prince A.** 2009. Ca2+ signaling in airway epithelial cells facilitates leukocyte recruitment and transepithelial migration. J. Leukoc. Biol. **86**:1135–1144.
12. **Chun J, Prince A.** 2009. TLR2-induced calpain cleavage of epithelial junctional proteins facilitates leukocyte transmigration. Cell Host Microbe **5**:47–58.
13. **Coussens PM, Colvin CJ, Wiersma K, Abouzied A, Sipkovsky S.** 2002. Gene expression profiling of peripheral blood mononuclear cells from cattle infected with Mycobacterium paratuberculosis. Infect. Immun. **70**:5494–5502.
14. **Derache C, et al.** 2009. Differential modulation of beta-defensin gene expression by Salmonella Enteritidis in intestinal epithelial cells from resistant and susceptible chicken inbred lines. Dev. Comp. Immunol. **33**:959–966.
15. **Eckmann L, Kagnoff MF.** 2005. Intestinal mucosal responses to microbial infection. Springer Semin. Immunopathol. **27**:181–196.
16. **Feldmeyer L, et al.** 2007. The inflammasome mediates UVB-induced activation and secretion of interleukin-1beta by keratinocytes. Curr. Biol. **17**:1140–1145.
17. **Gavrilin MA, Deucher MF, Boeckman F, Kolattukudy PE.** 2000. Monocyte chemotactic protein 1 upregulates IL-1beta expression in human monocytes. Biochem. Biophys. Res. Commun. **277**:37–42.
18. **Hines ME, II, Kreeger JM, Herron AJ.** 1995. Mycobacterial infections of animals: pathology and pathogenesis. Lab. Anim. Sci. **45**:334–351.
19. **Janagama HK, Jeong K, Kapur V, Coussens P, Sreevatsan S.** 2006. Cytokine responses of bovine macrophages to diverse clinical Mycobacterium avium subspecies paratuberculosis strains. BMC Microbiol. **6**:10.
20. **Janagama HK, et al.** 2010. Primary transcriptomes of Mycobacterium avium subsp. paratuberculosis reveal proprietary pathways in tissue and macrophages. BMC Genomics **11**:561.
21. **Kang PB, et al.** 2005. The human macrophage mannose receptor directs Mycobacterium tuberculosis lipoarabinomannan-mediated phagosome biogenesis. J. Exp. Med. **202**:987–999.
22. **Keshav S.** 2006. Paneth cells: leukocyte-like mediators of innate immunity in the intestine. J. Leukoc. Biol. **80**:500–508.
23. **Kohler H, et al.** 2007. Salmonella enterica serovar Typhimurium regulates intercellular junction proteins and facilitates transepithelial neutrophil and bacterial passage. Am. J. Physiol. Gastrointest Liver Physiol. **293**:G178–187.
24. **Koo IC, et al.** 2008. ESX-1-dependent cytolysis in lysosome secretion and inflammasome activation during mycobacterial infection. Cell Microbiol. **10**:1866–1878.
25. **Lamont EA, Sreevatsan S.** 2010. Paradigm redux—Mycobacterium avium subspecies paratuberculosis-macrophage interactions show clear variations between bovine and human physiological body temperatures. Microb. Pathog. **48**:143–149.
26. **Lim KB, et al.** 2008. The Cdc42 effector IRSp53 generates filopodia by coupling membrane protrusion with actin dynamics. J. Biol. Chem. **283**:20454–20472.
27. **Marchetti M, Sirard JC, Sansonetti P, Pringault E, Kerneis S.** 2004. Interaction of pathogenic bacteria with rabbit appendix M cells: bacterial motility is a key feature in vivo. Microbes Infect. **6**:521–528.
28. **Martinoli C, Chiavelli A, Rescigno M.** 2007. Entry route of Salmonella typhimurium directs the type of induced immune response. Immunity **27**:975–984.
29. **Mayer-Barber KD, et al.** 2010. Caspase-1 independent IL-1beta production is critical for host resistance to mycobacterium tuberculosis and does not require TLR signaling in vivo. J. Immunol. **184**:3326–3330.
30. **Meixenberger K, et al.** 2010. Listeria monocytogenes-infected human peripheral blood mononuclear cells produce IL-1beta, depending on listeriolysin O and NLRP3. J. Immunol. **184**:922–930.
31. **Michail SK, Halm DR, Abernathy F.** 2003. Enteropathogenic Escherichia coli: stimulating neutrophil migration across a cultured intestinal epithelium without altering transepithelial conductance. J. Pediatr. Gastroenterol. Nutr. **36**:253–260.
32. **Miltner E, et al.** 2005. Identification of Mycobacterium avium genes that affect invasion of the intestinal epithelium. Infect. Immun. **73**:4214–4221.
33. **Nobes CD, Hall A.** 1995. Rho, rac, and cdc42 GTPases regulate the assembly of multimolecular focal complexes associated with actin stress fibers, lamellipodia, and filopodia. Cell **81**:53–62.
34. **Patel D, et al.** 2006. The ability of Mycobacterium avium subsp. paratuberculosis to enter bovine epithelial cells is influenced by preexposure to a hyperosmolar environment and intracellular passage in bovine mammary epithelial cells. Infect. Immun. **74**:2849–2855.
35. **Pawlinski R, Setkowicz Z, Malodzinska K, Janeczko K.** 1999. Interleukin-1 beta affects the macrophage recruitment and proliferation in the injured brain of 6-day-old rat. Acta Neurobiol. Exp. (Warsaw) **59**:271–278.
36. **Rohrlich P, et al.** 1995. Interleukin-6 and interleukin-1 beta production in a pediatric plasma cell granuloma of the lung. Am. J. Surg. Pathol. **19**:590–595.

37. **Rumsey J, Valentine JF, Naser SA.** 2006. Inhibition of phagosome maturation and survival of Mycobacterium avium subspecies paratuberculosis in polymorphonuclear leukocytes from Crohn's disease patients. Med. Sci. Monit. **12**:BR130–BR139.
38. **Russell DG, Vanderven BC, Glennie S, Mwandumba H, Heyderman RS.** 2009. The macrophage marches on its phagosome: dynamic assays of phagosome function. Nat. Rev. Immunol. **9**:594–600.
39. **Sakaguchi T, Kohler H, Gu X, McCormick BA, Reinecker HC.** 2002. Shigella flexneri regulates tight junction-associated proteins in human intestinal epithelial cells. Cell Microbiol. **4**:367–381.
40. **Sanderson IR (ed).** 1999. Development of the gastrointestinal tract. Pmph USA Ltd., Shelton, CT.
41. **Sansonetti PJ.** 2001. Microbes and microbial toxins: paradigms for microbial-mucosal interactions III. Shigellosis: from symptoms to molecular pathogenesis. Am. J. Physiol. Gastrointest. Liver Physiol. **280**:G319–G323.
42. **Secott TE, Lin TL, Wu CC.** 2001. Fibronectin attachment protein homologue mediates fibronectin binding by Mycobacterium avium subsp. paratuberculosis. Infect. Immun. **69**:2075–2082.
43. **Secott TE, Lin TL, Wu CC.** 2002. Fibronectin attachment protein is necessary for efficient attachment and invasion of epithelial cells by Mycobacterium avium subsp. paratuberculosis. Infect. Immun. **70**:2670–2675.
44. **Secott TE, Lin TL, Wu CC.** 2004. Mycobacterium avium subsp. paratuberculosis fibronectin attachment protein facilitates M-cell targeting and invasion through a fibronectin bridge with host integrins. Infect. Immun. **72**:3724–3732.
45. **Sigurdardottir OG, Bakke-McKellep AM, Djonne B, Evensen O.** 2005. Mycobacterium avium subsp. paratuberculosis enters the small intestinal mucosa of goat kids in areas with and without Peyer's patches as demonstrated with the everted sleeve method. Comp. Immunol. Microbiol. Infect. Dis. **28**:223–230.
46. **Sluyter R, Shemon AN, Wiley JS.** 2004. Glu496 to Ala polymorphism in the P2X7 receptor impairs ATP-induced IL-1 beta release from human monocytes. J. Immunol. **172**:3399–3405.
47. **Souza CD, Evanson OA, Sreevatsan S, Weiss DJ.** 2007. Cell membrane receptors on bovine mononuclear phagocytes involved in phagocytosis of Mycobacterium avium subsp paratuberculosis. Am. J. Vet. Res. **68**:975–980.
48. **Srikanth CV, et al.** 2010. Salmonella pathogenesis and processing of secreted effectors by caspase-3. Science **330**:390–393.
49. **Sun SH.** 2010. Roles of P2X7 receptor in glial and neuroblastoma cells: the therapeutic potential of P2X7 receptor antagonists. Mol. Neurobiol. **41**:351–355.
50. **Sweet L, et al.** 2010. Mannose receptor-dependent delay in phagosome maturation by Mycobacterium avium glycopeptidolipids. Infect. Immun. **78**:518–526.
51. **Veterinary Record.** 2008. Johne's disease continues to be the most common cause of bovine enteric disease. Vet. Rec **163**:171–174.
52. **Wagner D, et al.** 2005. Elemental analysis of Mycobacterium avium-, Mycobacterium tuberculosis-, and Mycobacterium smegmatis-containing phagosomes indicates pathogen-induced microenvironments within the host cell's endosomal system. J. Immunol. **174**:1491–1500.
53. **Walker WS, IR.** 2007. TLRs in the gut. Am. J. Physiol. Gastrointest. Liver Physiol. **292**:G6–G10.
54. **Weiss DJ, Evanson OA, Souza CD.** 2005. Expression of interleukin-10 and suppressor of cytokine signaling-3 associated with susceptibility of cattle to infection with Mycobacterium avium subsp paratuberculosis. Am. J. Vet. Res. **66**:1114–1120.
55. **Welin A, et al.** 2008. Incorporation of Mycobacterium tuberculosis lipoarabinomannan into macrophage membrane rafts is a prerequisite for the phagosomal maturation block. Infect. Immun. **76**:2882–2887.
56. **Woo S, Heintz JA, Albrecht R, Barletta RG, Czuprynski CJ.** 2007. Life and death in bovine monocytes: The fate of Mycobacterium avium subsp. paratuberculosis. Microb. Pathog. **43**:106–113.
57. **Yamada H, Mizumo S, Horai R, Iwakura Y, Sugawara I.** 2000. Protective role of interleukin-1 in mycobacterial infection in IL-1 alpha/beta double-knockout mice. Lab. Invest. **80**:759–767.
58. **Zamudio-Meza H, Castillo-Alvarez A, Gonzalez-Bonilla C, Meza I.** 2009. Cross-talk between Rac1 and Cdc42 GTPases regulates formation of filopodia required for dengue virus type-2 entry into HMEC-1 cells. J. Gen. Virol. **90**:2902–2911.